

Size Effects on Droplet Displacing Process in Micropores by Multiscale Modeling

Fanli Liu* and Moran Wang[†]

Department of Engineering Mechanics
Tsinghua University, Beijing 100084, P. R. China
**liu-fl17@mails.tsinghua.edu.cn*
[†]mrwang@tsinghua.edu.cn

Received 13 June 2020

Accepted 26 July 2021

Published 28 August 2021

Transport mechanisms of small droplets on walls in micropores become significant for applications in energy, resource and biomedical engineering, however, a suitable numerical tool remains challenging. Macroscopic approach is ideal both in computing cost and simplicity but its applicability is doubted for nanoscale droplet, yet no clear evaluation on when exactly does it become invalid has been made. This work evaluates the applicability of macroscopic approach for the displacing process of droplet in a micropore and investigates relevant size effects, by comparing the simulation results of multiscale modeling and macroscopic method. Three types of size effects affecting the displacement results are identified: Laplace pressure, low interfacial density, and breakdown of macroscopic description. For the system studied, the Laplace pressure dominates for relatively big droplet, then low density region becomes significant for drop diameter smaller than 18 times molecule diameter, and finally macroscopic description gradually fails for drop diameter smaller than 13 times molecule diameter. We further investigate the influences of system scale and fluid type on these size effects and discuss the relative importance of each size effect under different conditions. Results indicate that traditional macroscopic approach may be invalid even when continuum assumption still holds due to other size effects, and corrections for those effects can be made to extend the applicability of macroscopic method.

Keywords: Size effect; droplet displacement; unconventional oil recovery; multiscale simulation.

1. Introduction

Oil may exist as nano-droplets massively attached to rock walls of micro-pores in many unconventional oil reservoirs, and oil recovery by flooding is essentially a process of displacing tiny droplet in a micro-pore by another fluid.¹ Investigating such process can help understand the underlying transport mechanism and possibly benefit not only oil industry but also other fields where similar phenomena exist.^{2–5} Choosing the suitable numerical tools for such process, however, leads to another problem. There are lots of studies on macroscale drop displacement,^{6–10} but the

[†] Corresponding author.

applicability of traditional macroscopic approach is generally doubted for such tiny oil droplet that its transport details may not be captured and continuum assumption may break down.¹¹ Purely microscopic approach, like molecular dynamics (MD), is not suitable either because the scale of the channel is in the order of a few micrometers, making MD unacceptably expensive in computational cost and unnecessary. In recent decades, researchers have developed a multiscale hybrid modeling method to resolve the dilemma.¹² The idea of multiscale hybrid modeling dates back to 1995 when O'Connell and Thompson proposed a domain decomposition scheme to couple different scales¹³ and since then lots of researchers have contributed in this field and improved the original algorithm.^{14–20} It is believed that the state-of-the-art multiscale tool can simulate such multiscale process correctly with affordable computing cost, but multiscale approach has its own drawback of being complex and much more time consuming than macroscopic method, which would be the most ideal approach if it still applies for nano-droplets.

Therefore, it would be helpful to know when exactly does macroscopic method fail and why. To the best knowledge of the authors, the specific size of the microscopic region in a general multiscale problem that makes macroscopic approach invalid has not been clarified in any previous work. In fact, some macroscopic method can achieve excellent agreement with MD down to nanoscale.^{21,22} Although it is well accepted that the limitation of resolution and the breaking of continuum assumption determine when macroscopic methods fail at molecular scale, some works suggest that even when the problem can be resolved by macroscopic method and continuum assumption still holds, certain size effects at small scale lead to incorrect results.²³ For the multiscale and multiphase displacing process where the strong interaction between droplet and flow adds to the complexity, possible size effects of the droplet has not been studied. Therefore, the aim of this work is to evaluate the applicability of macroscopic approach during droplet displacing process and investigate relevant size effects. The process of displacing droplet in a microchannel is simulated by both multiscale hybrid modeling and purely macroscopic method for monoatomic fluids with varying droplet sizes. Results by different approaches are compared to identify possible size effects. Then the influences of the system scale and fluid types on those size effects are studied. The relative significance of each size effect and possible corrections for macroscopic method to include those effects are also discussed.

2. Numerical Methods

2.1. *Physical model*

A two-dimensional model is adopted to represent the displacing process of droplet in a microchannel. As Fig. 1 shows, the system consists of two parallel plate walls with a droplet initially located on the center of the lower wall, and the bulk region is filled with another fluid. When simulation begins, the upper wall moves with a constant velocity to drive the bulk fluid, and droplet is displaced with the fluid flow.

In most cases, the height of the simulation domain between walls is 371.14 Å, the length 222.69 Å, and the upper wall velocity 94.75 m/s. The diameter of the droplet

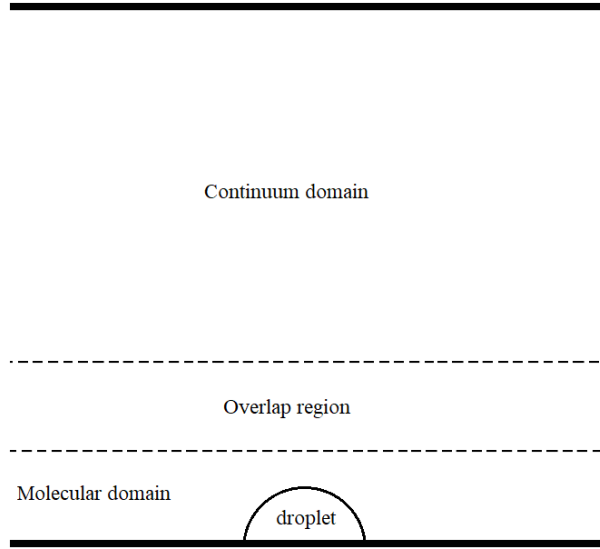


Fig. 1. Diagram of the simulation system. Droplet is initially located on the center of lower wall. The whole system is divided into two spatial domains, the molecular domain and the continuum domain, with an overlap region belonging to both domains.

is in the order of nanometer and is varied in different cases. Two systems of different fluids are studied: in the first system, liquid argon droplet is displaced by liquid argon at a bulk temperature of 120 K and pressure of 5 MPa, the interaction between droplet and bulk fluid is modified to achieve phase separation, while in the second system liquid n-butane droplet is displaced by water at 300 K and 4 MPa. Other parameters and boundary conditions for different methods are introduced in following sections.

2.2. Multiscale hybrid modeling

2.2.1. Domain decomposition

In a multiscale approach, as Fig. 1 illustrates, the simulation system is divided into two spatial domains, the molecular domain and the continuum domain. MD simulation is performed in the molecular domain, while lattice Boltzmann method (LBM) is adopted in the continuum domain. In the overlap region that belongs to both molecular and continuum domain, both types of simulations are performed. Coupling scheme for both scales in the overlap region is the key of this algorithm. Details of those methods are introduced in following sections.

2.2.2. MD in the molecular domain

As indicated by Fig. 1, MD is used to simulate the part of the system where the distance to the lower wall is smaller than 111.343 \AA to capture the molecular details

near the droplet. Argon and silicon walls are respectively adopted for the argon–argon system and butane–water system, with the interaction between walls and fluids modified to mimic no-slip boundary condition. The Lennard-Jones parameters of simple wall and fluid atoms are listed in Table 1. The SPC/E model is used for water, while a coarse-grained force field model for n-butane is introduced in Table 2,²⁴ where r is the distance between atoms, θ is the bond angle, and φ is the angle of torsion. The locations of atoms and mass centers of molecules are initialized in different FCC lattices, at densities under set temperature and pressure of corresponding system, which are listed in Table 3 along with other macroscopic properties.

Note that the z -direction, the direction perpendicular to the paper, has a finite length of 16 Å in MD simulation. Periodic boundary conditions are adopted in both x - and z -directions. The interface condition in y -direction in the overlap region will be introduced later. An NVE ensemble is used for the simulation and only temperature of fluids is maintained via a Nose–Hoover thermostat as the velocity of wall atoms is kept constant. Using a time step of 1 fs, the system is first relaxed with no external force and zero wall velocity for 3 ns, and then the displacing begins with a constant velocity assigned to upper wall for 16 ns. The density and displacement of

Table 1. Lennard-Jones parameters of simple wall and fluid atoms.

Atom type	Characteristic energy	Characteristic length	Cut off
Ar	119.8 K	3.41 Å	12 Å
Si	293.9 K	3.39 Å	12 Å

Table 2. Coarse-grained force field model for n -butane.

Physical aspect	Potential function	Parameters
Non-bonded interaction	$4\epsilon[(\frac{r}{\sigma})^{12} - (\frac{r}{\sigma})^6]$	$\sigma = 3.93 \text{ \AA}$ $\epsilon_{\text{CH}_3} = 114 \text{ K}$ $\epsilon_{\text{CH}_2} = 47 \text{ K}$
Bond stretching	$-\frac{H Q_0}{2} \ln[1 - (\frac{r-r_0}{Q_0})^2]$	$H = 96,500 \text{ K/\AA}^2$ $Q_0 = 1.572 \text{ \AA}$ $r_0 = 1.54 \text{ \AA}$
Bond bending	$\frac{1}{2} k_\theta (\theta - \theta_0)^2$	$k_\theta = 62,500 \text{ K/rad}^2$ $\theta_0 = 114^\circ$
Angle torsion	$[V_1(1 + \cos \varphi) + V_2(1 - \cos 2\varphi) + V_3(1 + \cos 3\varphi)]/2$	$V_1 = 355.03 \text{ K}$ $V_2 = -68.19 \text{ K}$ $V_3 = 701.32 \text{ K}$

Table 3. Macroscopic parameters used in simulation.

Macroscopic parameters	Argon-argon system	Butane-water system
Temperature	120 K	300 K
Pressure	5 MPa	4 MPa
Density	1191.6 kg/m ³	576.9 kg/m ³ (butane); 998.1 kg/m ³ (water)
Viscosity	118.8 $\mu\text{Pa} \cdot \text{s}$	163.7 $\mu\text{Pa} \cdot \text{s}$ (butane); 853.2 $\mu\text{Pa} \cdot \text{s}$ (water)
Interfacial tension	34.2 mN/s	63 mN/s
Contact angle	83.8°	77°

the droplet is calculated for further comparison. The result for each case is the average of eight cases that are identical except for the random number seed.

2.2.3. LBM in the continuum domain

As indicated by Fig. 1, LBM is used to simulate the part of the system where the distance to the lower wall is larger than 55.67 Å, where only the bulk fluid phase exists. The evolution equation for the distribution function is

$$f_i(\mathbf{x} + \mathbf{e}_i \Delta t, t + \Delta t) - f_i(\mathbf{x}, t) = -\frac{1}{\tau} [f_i(\mathbf{x}, t) - f_i^{\text{eq}}(\mathbf{x}, t)], \quad (1)$$

where $f_i(\mathbf{x}t)$ is the distribution function for the velocity vector \mathbf{e}_i in a standard D2Q9 lattice at place \mathbf{x} and time t , τ is the relaxation time, and the superscript in $f_i^{\text{eq}}(\mathbf{x}t)$ indicates it is the equilibrium distribution function, which is computed from the macroscopic density ρ and velocity \mathbf{u} as follows:

$$f_i^{\text{eq}} = \rho \omega_i \left[1 + \frac{3(\mathbf{e}_i \cdot \mathbf{u})}{c^2} + \frac{9(\mathbf{e}_i \cdot \mathbf{u})^2}{2c^4} - \frac{3(\mathbf{u} \cdot \mathbf{u})}{2c^2} \right], \quad (2)$$

where $c = \Delta x / \Delta t$ is the ratio of one grid length to one time step, and ω_i is the weighting factors defined as follows:

$$\omega_i = \begin{cases} \frac{4}{9}, & i = 0 \\ \frac{1}{9}, & i = 1, 2, 3, 4 \\ \frac{1}{36}, & i = 5, 6, 7, 8 \end{cases} \quad (3)$$

and macroscopic velocity and density can be obtained by the distribution functions:

$$\rho = \sum_{i=0}^8 f_i, \quad \rho \mathbf{u} = \sum_{i=0}^8 f_i \mathbf{e}_i. \quad (4)$$

Note that the macroscopic properties of fluids in Table 3 are used as input parameters for LBM. Periodic boundary condition is adopted in the x -direction, and bounce-back method is used at upper wall, which leads to no-slip condition for fluids. The interface condition in y -direction in the overlap region will be introduced later. The duration of LBM simulation is the same as MD, but with a much bigger time step, 500 fs, and a grid length of 18.56 Å.

2.2.4. Coupling in the overlap region

The coupling between scales is achieved by a Schwartz alternation method¹⁴: MD and LBM provide interface conditions for each other alternately in the overlap region. The interface conditions from MD to LBM are straightforward. Density and velocity for LBM is calculated by doing an average for particles within each

LBM grid:

$$\rho_J = \frac{1}{V} \sum_J m_i, \quad (5)$$

$$\rho_J \mathbf{u}_J = \frac{1}{V} \sum_J m_i \mathbf{u}_i, \quad (6)$$

where V is the volume of one grid, m_i and \mathbf{u}_i respectively the mass and velocity of the i th particle in grid J , ρ_J and \mathbf{u}_J respectively the macroscopic density and velocity obtained. Note that the time step in LBM is 500 times as one in MD, therefore, the interface density and velocity for LBM is the average of ρ_J and \mathbf{u}_J in previous 500 MD time steps.

The interface condition from LBM to MD is somehow tricky, as the state of particles is not uniquely determined by a few macroscopic parameters. A constraint method is used to make the mean particle velocity in grid J agree with the continuum solution, by modifying the total force exerted on each particle in grid J :

$$\dot{u}_i = \frac{F_i}{m_i} - \frac{1}{N_J m_i} \sum_{n=1}^{N_J} F_n + \frac{Du_J}{Dt}, \quad (7)$$

where \mathbf{F}_i is the total force exerted on the i th particle by all other particles, N_J is the number of particles in grid J , \mathbf{F}_n is the force exerted on the i th particle by the n th particle in grid J , and $D\mathbf{u}_J/Dt$ means the material derivative. For details, please refer to Ref. 16. The mass flux conservation is realized by adding or deleting particles in the overlap region according to the continuum velocity, as in Liu *et al.*'s work.¹⁶ Besides, additional interface condition is needed to prevent particles from entering the continuum domain. A newly proposed virtual wall scheme is adopted,²⁵ which has advantage over traditional method of preventing force²⁶ in that shear stress in the molecular domain is correct. More details about coupling in the overlap region can be found in our previous work.¹⁶

A single-phase Couette flow and a single-phase Poiseuille flow have been solved by our multiscale approach as a benchmark.²⁵ The evolutions of the velocity profile agree well with analytical solutions.

2.3. Purely macroscopic approach: Multiphase LBM

LBM can be applied to study a multiphase problem with suitable models. A Rothman–Keller-type model is adopted in our work to simulate the whole system.^{27,28} Two distribution functions need to be defined for the two fluid phases in our system. The relation between distribution functions and macroscopic properties and the evolution equations are indicated as follows:

$$\rho^{(k)} = \sum_i f_i^{(k)}, \quad \rho = \sum_k \rho^{(k)}, \quad \rho \mathbf{u} = \sum_k \sum_i f_i^{(k)} \mathbf{e}_i, \quad (8)$$

$$f_i^{(k)}(\mathbf{x} + \mathbf{e}_i \Delta t, t + \Delta t) - f_i^{(k)}(\mathbf{x}, t) = \Omega_i^{(k)}(f_i^{(k)}(\mathbf{x}, t)), \quad (9)$$

where the superscript k represents different phases and Ω stands for the collision term, which can be divided into two collision terms:

$$\Omega_i^{(k)} = -\frac{1}{\tau} (f_i^{(k)}(\mathbf{x}, t) - f_i^{(k),\text{eq}}(\mathbf{x}, t)) + \frac{A^{(k)}}{2} |\mathbf{F}| \left[\omega_i \frac{(\mathbf{e}_i \cdot \mathbf{F})^2}{|\mathbf{F}|^2} - B_i \right]. \quad (10)$$

The first collision term is similar to the single-phase BGK collision term except that the relaxation time in the multiphase region needs to be interpolated and the equilibrium distribution is calculated differently:

$$f_i^{(k),\text{eq}}(x, t) = \rho^{(k)} \left(C_i + \omega_i \left[\frac{3(\mathbf{e}_i \cdot \mathbf{u})}{c^2} + \frac{9(\mathbf{e}_i \cdot \mathbf{u})^2}{2c^4} - \frac{3(\mathbf{u} \cdot \mathbf{u})}{2c^2} \right] \right) + \Phi_i^{(k)}, \quad (11)$$

$$C_i = \begin{cases} \alpha^{(k)}, & i = 0 \\ \frac{1 - \alpha^{(k)}}{5}, & i = 1, 2, 3, 4, \\ \frac{1 - \alpha^{(k)}}{20}, & i = 5, 6, 7, 8 \end{cases}, \quad (12)$$

where α_k is a parameter adjusting the density ratios between two fluids and Φ_i^k is a correction term proposed by Leclaire *et al.*²⁷ In the second collision term, \mathbf{F} is the color gradient approximately perpendicular to the fluid interface, B_i is a fixed parameter, and A^k is a free parameter to determine the surface tension:

$$\mathbf{F} = \sum_i \mathbf{e}_i (\rho^{(1)}(\mathbf{x} + \mathbf{e}_i \Delta t) - \rho^{(2)}(\mathbf{x} + \mathbf{e}_i \Delta t)), \quad (13)$$

$$B_i = \begin{cases} -\frac{4}{27}, & i = 0 \\ \frac{2}{27}, & i = 1, 2, 3, 4, \\ \frac{5}{108}, & i = 5, 6, 7, 8 \end{cases}, \quad (14)$$

$$\sigma = \frac{(A^{(1)} + A^{(2)})\tau}{9} \sum_{\mathbf{x}} |\mathbf{F}|. \quad (15)$$

Usually a recoloring operator is used after collision and before streaming to achieve phase separation. The distribution functions after collision denoted by a superscript “*”, the recoloring algorithm has the following form:

$$f_i^{(1)} = \frac{\rho^{(1)}}{\rho} f_i^* + \beta \frac{\rho^{(1)}\rho^{(2)}}{\rho^2} \cos(\lambda_i) \sum_k f_i^{(k),\text{eq}}(\rho^{(k)}, 0, \alpha^{(k)}), \quad (16)$$

$$f_i^{(2)} = \frac{\rho^{(2)}}{\rho} f_i^* + \beta \frac{\rho^{(1)}\rho^{(2)}}{\rho^2} \cos(\lambda_i) \sum_k f_i^{(k),\text{eq}}(\rho^{(k)}, 0, \alpha^{(k)}), \quad (17)$$

where $\cos(\lambda_i) = \mathbf{e}_i \cdot \mathbf{F} / (|\mathbf{e}_i| \cdot |\mathbf{F}|)$.

Similar to the single-phase LBM, the macroscopic properties of fluids in Table 3 is used as input parameters. Different contact angles are achieved by assigning different densities to wall nodes. Periodic boundary condition is adopted in the x -direction, and bounce-back method is used at both walls, which leads to no-slip condition for fluids. The duration of multiphase LBM simulation is the same as multiscale hybrid modeling, and in order to resolve molecular scale, a grid length of 1.86 Å and a time step of 1.35 fs are adopted. The multiphase model has been benchmarked by a layered Couette flow with different density ratios.²⁹

2.4. Macroscopic correction for Laplace pressure

The interfacial tension will lead to a huge pressure difference across the curved surface of extremely small droplet, which is one possible size effect that invalidates macroscopic method, as the actual density and viscosity of droplet are different from those inputted and the method itself cannot capture well the change of properties due to huge pressure. However, it is possible to consider this effect beforehand. The relation between droplet size, density, and pressure difference is shown as follows:

$$P_{\text{drop}} - P_{\text{bulk}} = \frac{\sigma}{R}, \quad (18)$$

$$\rho_{\text{drop}} = \frac{M}{(\theta R^2 - R^2 \sin(2\theta)/2)L_y} R, \quad (19)$$

where ρ , R , M , and θ are respectively the density, radius, mass and contact angle of droplet, and L_y is the length in the y -direction of the simulation domain. Given the mass and original input size of the droplet, the pressure inside the droplet is calculated and the corresponding density at this pressure can be found in NIST.³⁰ The actual size of droplet is obtained by adjusting the input size until the theoretical density agrees with the density calculated from input size. By using the actual size and corresponding fluid properties as input parameters, the change due to Laplace pressure is captured. Note that this correction is only exact for fluids in equilibrium and will have deviations during a dynamic process.

3. Results and Discussion

This section consists of three parts. First, possible size effects are identified in an argon–argon system by comparing multiscale hybrid modeling and purely macroscopic simulation results with varying droplet size. Then, the influences of the scale of the whole system on size effects are studied. Finally, size effects in a system made up of more realistic fluids, the butane–water system, are investigated.

3.1. Size effects in an argon–argon system

Figure 2 illustrates the droplet displacement by multiscale hybrid modeling, multiphase LBM without correction for Laplace pressure, and multiphase LBM with

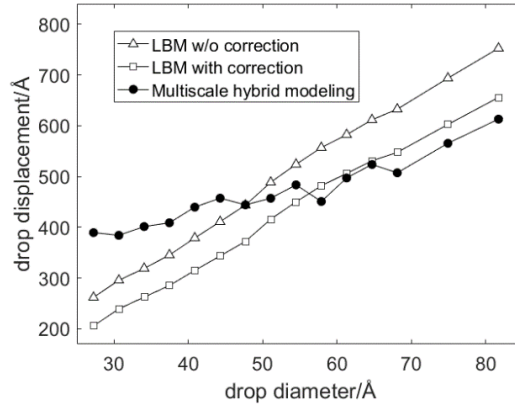


Fig. 2. Drop displacement against varying drop sizes in argon–argon system obtained by different methods.

correction against different droplet diameters. Here, “droplet displacement” means the displacement of the center of mass of the drop. The results clearly show that the effects of Laplace pressure for droplet diameter are larger than 60 Å: the displacement by purely macroscopic method without correction deviates more than 20% from multiscale hybrid modeling as both the actual density and viscosity of droplet are larger due to Laplace pressure, while the deviation after correction is within 5%. However, as the droplet size decreases further, the correction starts to fail as well and the displacement by multiscale hybrid modeling becomes closer to the uncorrected case, eventually surpassing it. For the smallest drop size in our simulation, the multiscale displacement is almost 50% more than macroscopic result, with or without pressure correction. This abnormality indicates that some other effects must be in play. A similar trend can be found by examining the density of droplet in different simulations, as Fig. 3 shows. Note that the droplet density in multiscale hybrid modeling is obtained by doing space and time average after relaxation, whereas the density in multiphase LBM is the input density as it is almost a constant during simulation. When the droplet size is rather big, the increase of density due to pressure difference is evident. As the droplet diameter gets smaller than 60 Å, the density begins to decrease, but still larger than uncorrected case. Eventually the density of droplet in multiscale simulation becomes a bit smaller than the uncorrected value. The density curve corresponds to the displacement results as droplet displacement becomes larger as its density decreases.

One possible cause for the abnormal decrease of density for small droplet size is the low local density in the interface region.^{31,32} Figure 4 illustrates the local density of the two fluids in our simulation system near a planar interface obtained by MD. Near the interface, the local density of both fluids has a sharp decrease to almost zero. For a big drop, the interface region only takes up a negligible part of the whole droplet, therefore it has no effect on the drop density. Once the drop diameter gets

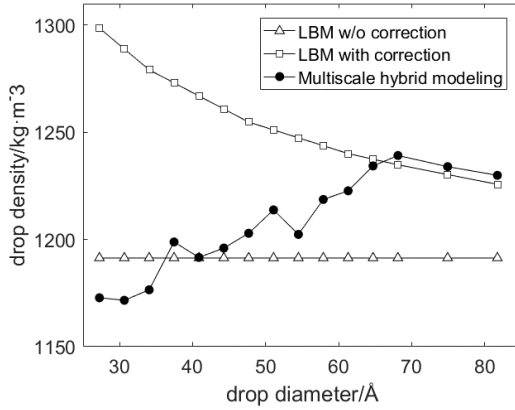


Fig. 3. Drop density against varying drop sizes in argon-argon system obtained by different methods.

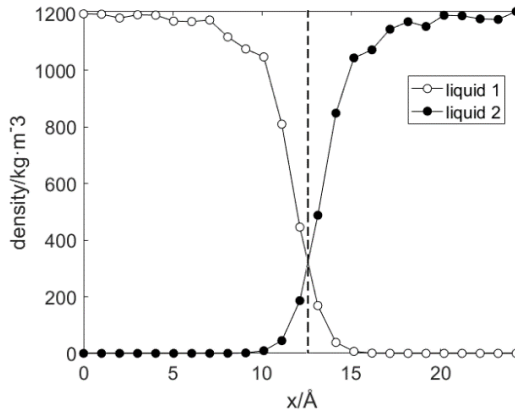


Fig. 4. Local density of fluids in our simulation system near a planar interface indicated by the dashed line.

small enough that the width of the interface region is no longer negligible, the effective density of the drop will become smaller than the bulk value due to the low local density region. Lower effective density leads to lower viscosity, and they both contribute to the larger droplet displacement. According to Fig. 4, the low local density region thickness is estimated as 2 Å, for a droplet of diameter 60 Å, the percentage of this region is approximately $(30^2 - 28^2)/30^2 = 12.9\%$, which indeed will have a considerable influence on droplet density.

Still, the macroscopic method can be extended to include this low density region effect through an upscaling algorithm, namely using the actual density and viscosity obtained from MD as input parameters, which makes it a multiscale approach. Although substituting one average density for an inhomogeneous density distribution might be problematic, the upscaling results in Fig. 5 show that it does somehow

Size Effects on Droplet Displacing Process in Micropores by Multiscale Modeling

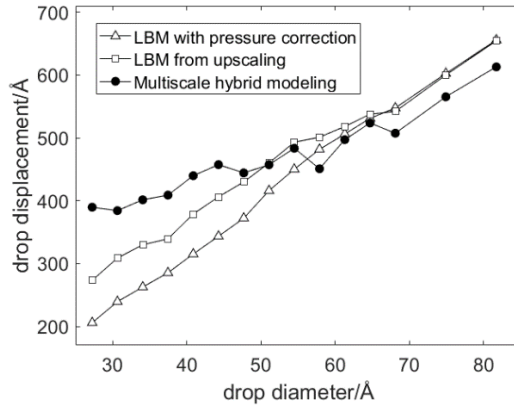


Fig. 5. Drop displacement against varying drop sizes in argon–argon system by upscaling compared with other methods. Results show that upscaling compensates for the low density region effect over a certain range.

compensate for those size effects for a certain range until droplet diameter gets smaller than 45 Å. The upscaling approach also becomes invalid when the drop size decreases further. This is within expectation as the macroscopic constitution relation no longer holds for extremely small scale, and even the act of defining macroscopic variables for this tiny droplet is doubtful. This last effect is generally recognized as the primary reason for abandoning pure macroscopic approaches for a multiscale problem in previous works.

3.2. Influences of system scale on size effects

Previous studies have suggested that the molecular region has few effect on the continuum region far enough.²¹ This can be readily seen in Fig. 6, which shows that the velocity profiles in the upper part of the continuum region are almost identical in

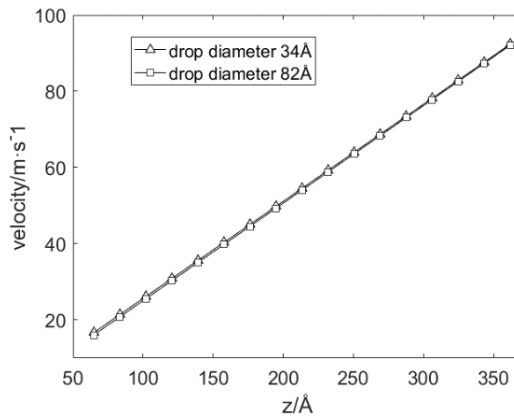


Fig. 6. Velocity in the continuum domain for two different drop sizes.

spite of different droplet sizes. Since the interaction between the molecular region and far end of the continuum region is weak, it is possible to investigate size effects with a smaller system to save computational cost. The influences of system scale on size effects are studied by simulating the same displacing process with the length in z -direction shrunk to one-third of the original value. The density and displacement results are illustrated in Figs. 7 and 8. Although there is quantitative difference, the trend is similar to that in a larger system: Laplace pressure effect dominants for larger droplet, then the low local density region becomes significant as drop size decreases, and finally macroscopic description breaks down. Therefore, when studying size effect qualitatively, we can use a smaller simulation domain for simplicity.

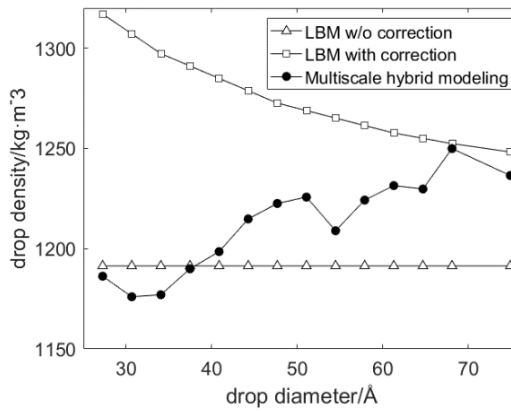


Fig. 7. Drop density against varying drop sizes in smaller argon–argon system obtained by different methods.

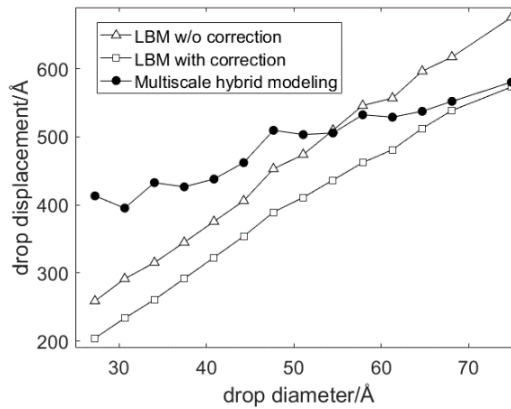


Fig. 8. Drop density against varying drop sizes in smaller argon–argon system obtained by different methods.

3.3. Influences of fluid type on size effects

We further simulate the same displacing process in a system consisting of more realistic fluids, butane as the droplet and water as the bulk flow, to investigate the impact of fluid type on size effects. A smaller simulation domain mentioned in the previous section is adopted for the butane–water system. The density and displacement results are shown in Figs. 9 and 10. The same size effects can be observed in the density curve: for bigger drop, the density from MD agrees with macroscopic value after Laplace pressure correction, then with smaller drop there is an abnormal decrease likely due to the low density interface region. As for the displacement curve, although the trend is similar in the sense that the results of MD and LBM do agree better for bigger drop and deviation becomes larger as droplet size decreases, the

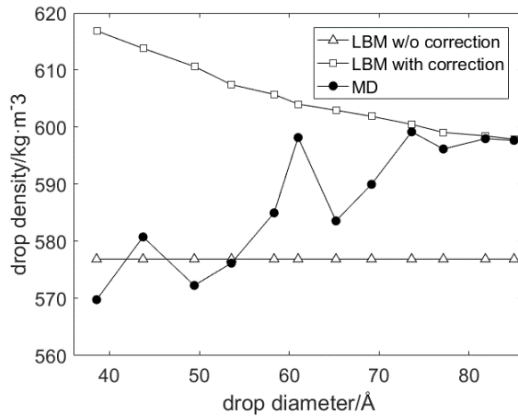


Fig. 9. Drop density against varying drop sizes in butane–water system obtained by different methods.

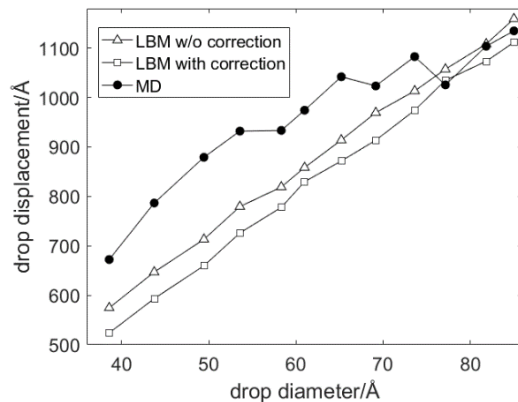


Fig. 10. Drop displacement against varying drop sizes in butane–water system obtained by different methods.

displacement by MD is generally larger than expected. For a butane droplet of diameter 70 Å, the MD density is between the corrected and uncorrected macroscopic value, but the MD displacement is the largest of those three, which indicates that, unlike the argon–argon system, upscaling fails very early. We argue that this is not likely because the macroscopic description has already broken down, as the 70 Å droplet consists of 224 butane molecules which is enough to yield meaningful macroscopic properties. One important difference between butane and argon is that butane fluid has more profound shear-thinning effect,³³ which might account for the larger displacement of butane droplet.

Although it is still far from the conclusion that similar trend of size effects exists for all fluid types, some simple theoretical analysis can be made. The Laplace pressure effect is dependent on the interfacial tension and the sensitivity of droplet density and viscosity to pressure. For the two fluid systems in our work, this effect emerges the earliest, but if the interfacial tension is very small due to surfactants, the pressure difference across the interface could be negligible even for tiny droplet, therefore eliminating this size effect. The thickness of the low density region is weakly related to the molecule size, therefore the scale where low density region effect becomes significant should be similar for most common fluids, whose molecule sizes do not differ a lot. The same applies to the scale where macroscopic description breaks down. Droplet made up of much larger fluid molecules contains much fewer molecules for the same drop size, so macroscopic relation will fail earlier. In other aspects, this effect should be invariant of fluid type.

4. Conclusion

This paper evaluates the applicability of macroscopic approach during droplet displacing process in micropores. We investigate the relevant size effects by comparing the simulation results of multiscale hybrid modeling and purely macroscopic method for varying droplet sizes. First, three types of size effects are identified. In addition to the breakdown of macroscopic description which is generally accepted as the primary reason that invalidates purely macroscopic methods, two other size effects, the Laplace pressure difference and the low local density near interface region, are also identified and proved to affect the displacement results. For the system studied in our work, the Laplace pressure effect emerges the earliest, then the low local density region becomes non-negligible when drop diameter is decreased to 60 Å, about 18 times the molecule diameter, and finally macroscopic description gradually breaks down as drop diameter gets smaller than 45 Å, about 13 times the molecule diameter. Therefore, traditional macroscopic approach may fail even before the breakdown of continuum assumption. Second, we investigate the influences of system scale and fluid type on these size effects. Results show that it is possible to study size effects qualitatively with a smaller system as it shows the exact same trend as in the bigger system. Similar size effects exist for other fluid types, but their relative significance may be different. The Laplace pressure effect is dependent on the interfacial tension

and the sensitivity of fluid density and viscosity to pressure, thus can be weakened if surfactants are added. The scale where low density region becomes significant and where macroscopic description breaks down is thought to be almost invariant of fluid type except for fluid consisting of very large molecules, in which case the breakdown happens earlier. Lastly, we also show possible corrections to extend the applicability of macroscopic approach. In our study, Laplace pressure effect is considered beforehand by estimating the actual drop size and fluid properties as input parameters, and low density in the interface region is captured by an upscaling algorithm with the help of MD. Theoretical correction for the low interfacial density effect may also be possible if the interfacial density profile can be obtained by macroscopic analysis.

Acknowledgments

This work is financially supported by the NSF grant of China (No. U1837602, 91634107) and the National Key Research and Development Program of China (No. 2019YFA0708704).

References

1. J. Bear, *Dynamics of Fluids in Porous Media* (Courier Corporation, 2013).
2. R. Baviere, J. Boutet and Y. Fouillet, Dynamics of droplet transport induced by electrowetting actuation, *Microfluid. Nanofluid.* **4**(4) (2008) 287–294.
3. J.-M. Roux, Y. Fouillet and J.-L. Achard, 3D droplet displacement in microfluidic systems by electrostatic actuation, *Sens. Actuators A: Phys.* **134**(2) (2007) 486–493.
4. D. L. Reichard, Drop formation and impaction on the plant, *Weed Technol.* **2**(1) (1988) 82–87.
5. H. Nomura *et al.*, Microgravity experiments on droplet motion during flame spreading along three-fuel-droplet array, *Proc. Combust. Inst.* **32**(2) (2009) 2163–2169.
6. Q. Kang, D. Zhang and S. Chen, Displacement of a two-dimensional immiscible droplet in a channel, *Phys. Fluids* **14**(8) (2002) 3203–3214.
7. Q. Kang, D. Zhang and S. Chen, Displacement of a three-dimensional immiscible droplet in a duct, *J. Fluid Mech.* **545** (2005) 41–66.
8. H. N. Joensson, M. Uhlén and H. A. Svahn, Droplet size based separation by deterministic lateral displacement — separating droplets by cell-induced shrinking, *Lab Chip* **11**(7) (2011) 1305–1310.
9. P. Randive, A. Dalal and P. P. Mukherjee, Probing the influence of superhydrophobicity and mixed wettability on droplet displacement behavior, *Microfluid. Nanofluid.* **17**(4) (2014) 657–674.
10. P. Randive and A. Dalal, Influence of viscosity ratio and wettability on droplet displacement behavior: A mesoscale analysis, *Comput. Fluids* **102** (2014) 15–31.
11. D. Grecov, L. de Andrade Lima and A. Rey, Multiscale simulation of flow-induced texture formation in polymer liquid crystals and carbonaceous mesophases, *Mol. Simulat.* **31**(2–3) (2005) 185–199.
12. S. Chen, M. Wang and Z. Xia, Multiscale fluid mechanics and modeling, *Procedia IUTAM* **10** (2014) 100–114.
13. S. T. O’connell and P. A. Thompson, Molecular dynamics–continuum hybrid computations: A tool for studying complex fluid flows, *Phys. Rev. E* **52**(6) (1995) R5792.

14. N. G. Hadjiconstantinou and A. T. Patera, Heterogeneous atomistic-continuum representations for dense fluid systems, *Int. J. Mod. Phys. C* **8**(4) (1997) 967–976.
15. E. Flekkøy, G. Wagner and J. Feder, Hybrid model for combined particle and continuum dynamics, *Europhys. Lett.* **52**(3) (2000) 271.
16. J. Liu, S. Chen, X. Nie and M. O. Robbins, A continuum–atomistic simulation of heat transfer in micro-and nano-flows, *J. Comput. Phys.* **227**(1) (2007) 279–291.
17. J. Liu, S. Chen, X. Nie and M. O. Robbins, A continuum-atomistic multi-timescale algorithm for micro/nano flows, *Commun. Comput. Phys.* **4**(5) (2008) 1279–1291.
18. X. Nie, S. Chen and M. Robbins, A continuum and molecular dynamics hybrid method for micro-and nano-fluid flow, *J. Fluid Mech.* **500** (2004) 55–64.
19. G. Wagner and E. Flekkøy, Hybrid computations with flux exchange, *Philos. Trans. A: Math., Phys. Eng. Sci.* **362**(1821) (2004) 1655–1665.
20. R. Delgado-Buscalioni, Tools for multiscale simulation of liquids using open molecular dynamics, in *Numerical Analysis of Multiscale Computations* (Springer, 2012), pp. 145–166.
21. J. Horbach and S. Succi, Lattice Boltzmann versus molecular dynamics simulation of nanoscale hydrodynamic flows, *Phys. Rev. Lett.* **96**(22) (2006) 224503.
22. S. Succi, A. Mohammad and J. Horbach, Lattice–Boltzmann simulation of dense nano-flows: a comparison with molecular dynamics and Navier–Stokes solutions, *Int. J. Mod. Phys. C* **18**(4) (2007) 667–675.
23. H. Tian, W. Huang, M. Li and M. Wang, Critical size of continuum theory applicability for single-phase liquid flow in nanochannel, *J. Nanosci. Nanotechnol.* **17**(8) (2017) 6149–6158.
24. R. Khare, J. de Pablo and A. Yethiraj, Rheological, thermodynamic, and structural studies of linear and branched alkanes under shear, *J. Chem. Phys.* **107**(16) (1997) 6956–6964.
25. G. Liu, J. Zhang and M. Wang, Drop movements and replacement on surface driven by shear force via hybrid atomistic–continuum simulations, *Mol. Simulat.* **42**(9) (2016) 855–862.
26. W. Zhou, H. Luan, Y. He, J. Sun and W. Tao, A study on boundary force model used in multiscale simulations with non-periodic boundary condition, *Microfluid. Nanofluid.* **16**(3) (2014) 1.
27. S. Leclaire, N. Pellerin, M. Reggio and J.-Y. Trépanier, Enhanced equilibrium distribution functions for simulating immiscible multiphase flows with variable density ratios in a class of lattice Boltzmann models, *Int. J. Multiphase Flow* **57** (2013) 159–168.
28. S. Leclaire, M. Reggio and J.-Y. Trépanier, Numerical evaluation of two recoloring operators for an immiscible two-phase flow lattice Boltzmann model, *Appl. Math. Model.* **36**(5) (2012) 2237–2252.
29. C. Xie, J. Zhang, V. Bertola and M. Wang, Lattice Boltzmann modeling for multiphase viscoplastic fluid flow, *J. Non-Newtonian Fluid Mech.* **234** (2016) 118–128.
30. E. Lemmon, M. McLinden, D. Friend, P. Linstrom and W. Mallard, NIST chemistry WebBook, Nist standard reference database number 69, National Institute of Standards and Technology, Gaithersburg (2011).
31. A. R. Van Buuren, S. J. Marrink and H. J. Berendsen, A molecular dynamics study of the decane/water interface, *J. Phys. Chem.* **97**(36) (1993) 9206–9212.
32. S. Iatsevitch and F. Forstmann, Density profiles at liquid–vapor and liquid–liquid interfaces: An integral equation study, *J. Chem. Phys.* **107**(16) (1997) 6925–6935.
33. S. H. Lee and P. T. Cummings, The rheology of n-butane and i-butane by non-equilibrium molecular dynamics simulations, *Mol. Simulat.* **16**(4–6) (1996) 229–247.